

Integrating spatial analytics in power system planning techniques for the green energy transition

Keagen Liebenberg ^{a,*}, Sanjian Malapermal ^a

^a Eskom Holdings SOC Ltd; liebenk@eskom.co.za, malapes@eskom.co.za

* Corresponding author

Abstract: Fossil fuel energy generation contributes significantly to greenhouse gas emissions globally. Energy transition towards sustainable, low-carbon energy needs to occur. South Africa has pledged to achieve a net-zero carbon economy by 2050 and in-line with this energy transition. The country has implemented the Renewable Energy Independent Power Procurement Programme (REIPPPP) to promote private investment within the energy sector. As new capacity is constructed, it requires the national grid to move from a vertically integrated passive power model to a deregulated active power flow due to the distributed sources of energy. In this paper, a method for connecting distributed power producers is introduced by providing candidate locations for Network Planners to develop insights for optimal placement of collector stations that connect multiple power producers in an orderly manner onto the electrical grid. This method uses buffer distances and Voronoi polygons from the stations on the national grid in order for the power producers to be aggregated and assigned connection to a collector station. Furthermore, this paper proposes a model for potential power producers that allows Network Planners to adequately plan for future grid access applications.

Keywords: energy transition, spatial analysis, renewable energy, PyQGIS, green energy transition

1. Introduction

Global temperatures have been increasing since 1880, with a rise in anthropogenic sources of greenhouse gases being the primary cause of this increase (Asif, 2022). It is difficult to predict the effect this rise in global temperatures has on the planet. It is generally accepted that climate change leading to extreme weather events and abnormalities has been one of the major consequences. Much work has gone into creating global awareness and cooperation amongst nations to limit the rise in global temperatures. Greenhouse gas emissions due to human-activity globally have continued to increase during the second decade of the 21st century (IPCC, 2022). As the majority of greenhouse gas emissions can be attributed to fossil fuel energy generation, this sector requires an urgent transition to non-greenhouse gas emitting energy sources (Covert et al., 2016). The transition to sustainable, low-carbon energy sources has four key dimensions: decarbonisation, decentralisation, deregulation and digitalisation (Asif, 2022).

With regards to South Africa, the country accounts for 1% of global CO₂ emissions (Mashishi, 2021) and have pledged to achieve a net-zero carbon economy by 2050 (IPCC, 2022). Decarbonisation for South Africa means planning for an energy transition away from fossil fuel energy sources – which by 2030 will make up 58.8% of the country's energy mix (Department of Mineral Resources and Energy, 2019) – to carbon neutral ones. The country's largest utility is now struggling to maintain an

aging coal fleet in an environment where lenders are becoming increasingly opposed to financing coal-fired power stations (Chan et al., 2022). However, financial institutions are readily offering finance for investment in a decarbonisation energy transition (World Bank, 2022). South Africa is also rich in energy sources and has ample potential sources of renewable energy to utilise in this transition (NPC, 2011).

In line with South Africa's Integrated Resource Plan (IRP) published in 2019, the country implemented the Renewable Energy Independent Power Producer Procurement Programme (REIPPPP) (Ayamolowo et al., 2022). The REIPPPP is a competitive bidding process that promotes private sector investment in grid-connected renewable energy within South Africa (Naicker and Thopil, 2019). As a result of this programme, there has been 5323.9MW of renewable energy capacity that has been installed within the country between 2016 and 2021 (Ayamolowo et al., 2022). In addition to this, REIPPPP bid window 5 resulted in the signing of 13 preferred bidder projects totalling 975MW with the preferred bidders for bid window 6 totalling 860MW (Department of Mineral Resources and Energy, 2022).

With all this new capacity being constructed due to the push for the decarbonisation of South Africa's energy sources, the new capacity will also be decentralised – with many smaller renewable energy power stations compared to the fossil fuel powered stations currently producing the majority of the electricity in South Africa (Department of Mineral Resources and Energy, 2019). The country's coal-

fired power stations are located in the northeast of the country while South Africa's renewable energy potential is greatest in the northwest (solar) (Suri et al., 2020) and the south (wind) (Floors and von Saint Ange, 2021). This presents a challenge from a grid planning point-of-view, where power traditionally flowed from a central pool in the northeast of the country, through a vertically integrated regulated passive power model, to a very deregulated active power flow (Eskom, 2021). The consequence of which requires multiple infrastructure upgrades to support the new distributed sources of energy (Matshidza et al., 2022). Unlike the previous power model that optimized the network as the power requirements tapered off closer to the load. The new deregulated power-model requires strengthening with each additional megawatt that is supplied from the distributed deregulated source, to ensure sufficient evacuation of the energy to the grid.

With regards to the shift in energy generation, not only in South Africa but around the world, a new approach needed to be formulated that would allow network planners to plan the connection of numerous entrants onto the electricity grid. This involves mapping the location of the prospective independent power producers (IPPs) and connecting them to an existing electrical station, considering future applications. Providing candidate locations for Network Planners to develop insights for optimal placement of collector stations (i.e. aggregators) to conscientiously connect multiple IPPs in an orderly manner to evaluate the renewable power to the grid. This presented two problems, namely: knowing which areas are being targeted by IPPs and strategies of connecting them onto the electricity network. These challenges will be dealt with in this paper.

2. Mapping prospective IPPs

This first challenge that was dealt with was to estimate the location and potential capacity (megawatts to be installed) that prospective IPPs are investigating installing within South Africa. This was handled by utilising the South African Renewable Energy EIA Application (REEA) Database, which includes the spatial and attribute information regarding renewable energy applications for environmental authorisation (DFFE, 2022). The attribute information includes the potential capacity that the Network Planners needed to plan.

This dataset is managed by the Department of Forestry, Fisheries and the Environment (DFFE) within the South African government and approves the EIA as required for the construction of renewable energy projects – as mandated by the relevant Act (Department of Environmental Affairs, 2013). Therefore, this dataset was a good indicator of the potential capacity to be developed as well as the location of these projects.

2.1 Data processing

The REEA_OR_2021_Q2 version of this dataset was downloaded from the DFFE GIS data catalogue website and used for this assessment (DFFE, 2022). As this dataset included a row for every assessment logged as well as amendments per project, the duplicates needed to be

managed in order to display uniqueness in the dataset per renewable energy project application. This was done by removing the entries where status under the "PRJ_STATUS" column was "Withdrawn/Lapsed" and then by creating a unique project number from the "DEA_REF" column by extracting the largest number using a variety of text extraction techniques in Microsoft Excel. The date in the "APP_RECEIV" column was also used to extract the latest application submitted per project. If this entry did not have a value present in the "MEGAWATT" column (if this column was left blank or had a value of 0) then regular expressions (Regex) were used to find possible megawatts mentioned in the "PROJ_TITLE" column. The remaining entries that had no "MEGAWATT" value were assigned a "MEGAWATT_LOWER" value of 75 and a "MEGAWATT_HIGHER" value of 100, based on the averages of the dataset. This would allow the Network Planner to decide on their modelling path.

3. Development of the collector strategy

After the prospective IPPs dataset was created, a strategy was developed to follow the connection of these IPPs to the electricity grid (Jaglal, 2016). In order to develop this strategy, it was determined that 100km was the maximum distance an IPP could be located from a main transmission station – any IPP further than this maximum would be flagged as significantly far for any effective solution. This analysis was performed on the South African Transmission network stations – with the points of connection being the main transmission stations.

3.1 Collector stations

A collector station is planned for a maximum of 500MW of capacity connected to it with a maximum distance of 30km from the Main Transmission Station (MTS) (Jaglal, 2016). A single IPP, less than 200MW, should ideally not be connected directly to an MTS. A collector station should ideally be planned to collect and aggregate multiple IPPs and transmit the aggregated energy to the main transmission station. Satellite-stations aggregate IPPs that are located between 30-100km from an MTS and connect to a collector. A satellite station is located between 30-60km from an MTS. While a network impedance model is the best proxy for identifying the ideal location for a collector station, it was not considered in this paper but remains a long-term goal for this study. Figure 1 illustrates this diagrammatically.

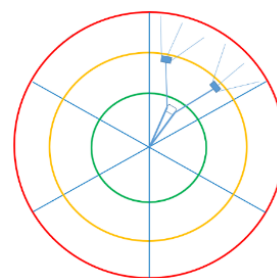


Figure 1: The collector strategy showing the buffer zones at various distances with a collector station from the central station with further satellite stations at distances greater than 30km

3.2 Software environment

The end-state for the model in this study was to be a toolset for Network Planners with a Graphical User Interface (GUI) where changes to the input datasets as well as edits to the collector distances described in 3.1 can be made. QGIS was chosen to develop the toolset because it is a free and open source GIS application that doesn't require expensive software licences.

Initially, the QGIS Graphical Modeller was used which has a drag and drop interface. However, the limitations of this QGIS component became apparent, in particular the functionality to iterate and select different features within a dataset. Therefore, it was decided to transition to Python for this study, specifically the QGIS Python module (PyQGIS). Using this module within QGIS enabled the output to be rendered to the map canvas after the tools were run. QGIS is packaged with a script template for python and allows the scripter to create a GUI, which was used for the creation of the tools in this study.

3.3 Creation of buffer zones

The collector strategy adopted different tactics in dealing with connecting the prospective IPPs depending on their distance from the stations. These distances represent a broad graduation approach, whereby 3 bands of graduation distances are used as a one-third approach. However, future work will use this broad approach to identify finer graduations that may fit 5 or 10 bands of 0-20km or 0-10km respectively, where there is a high concentration of renewables. The proposed distances for the 3 bands of graduation in the broad approach are itemised below and are editable in range as a user selection:

1. 0-30km: position of a collector station and was colour coded as green as IPPs are easiest to connect in this area.
2. 30-60km: position of a satellite station and was colour coded as orange.
3. 60-100km: region where it will be difficult to connect IPPs and was colour coded as red.

Figure 2 illustrates the process flow that was followed creating the buffer zones. The input datasets for this process were the stations to be used as grid connections and provinces for the province name and a final clip on the buffer zones. The first step was to reproject the input datasets to a project coordinate system – as there was a need for distance calculations in metres. EPSG:9221 – Hartebeesthoek94 / ZAF BSU Albers 25E was used in the study as it met the criteria and it covered the whole of South Africa, unlike the transverse Mercator coordinate system used by mapping agencies in the country which has multiple bands across the country.

A spatial join was performed between the reprojected stations and provinces to join the province name attribute to the station's dataset. Buffer zones were then created around the stations using the distances supplied by the user (the default was 30km, 60km and 100km). The symmetrical difference was then used to "cut out" the buffers so that the 30-60km and 60-100km buffer zones

were doughnuts; the reason being so that when these are eventually joined to the IPPs there are no duplicates.

There was a specific requirement for the buffer zones to be located within the Voronoi polygon of a given station. Voronoi polygons, also referred to as Thiessen polygons, have locations within the shape that are the same value as the nearest point, namely the stations in this study (Bolstad, 2008). These Voronoi polygons were created for the input stations and once the difference tool was run on the buffers, all buffer distances were merged and an intersect performed between the Voronoi polygons and merged buffers. Duplicates were removed from the intersection and the result was clipped by the provinces boundary and exported from the processing algorithm. The result of this process using the main transmission stations in South Africa as the input stations is shown in Figure 3.

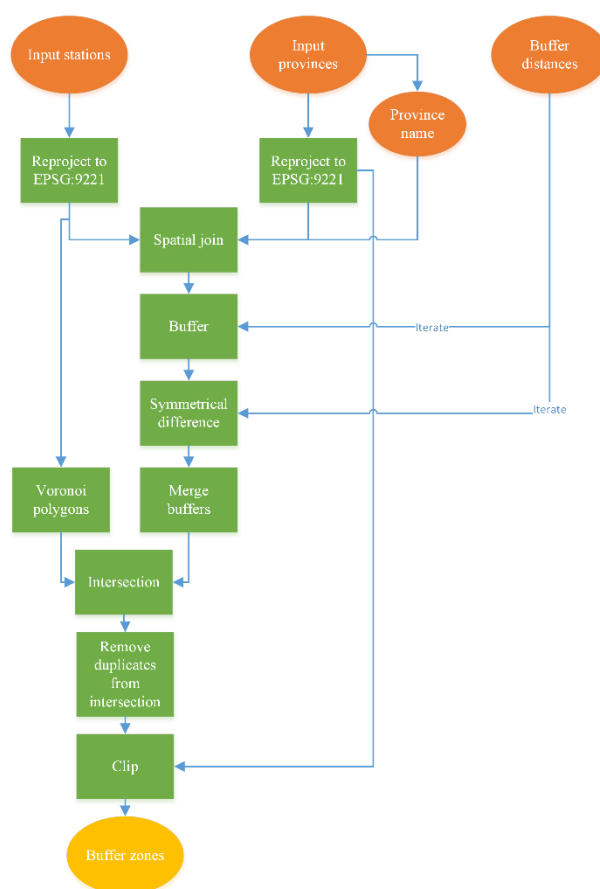


Figure 2: The process flow used to create the buffer zones

3.4 Creation of buffer zone segments

Following the creation of the buffer zones, a second layer of scaffolding is required to create a sector-based-positioning of the applications. This layer is instrumental in aggregating inputs for the positioning of candidate collector sites within a station's buffer zones. The second layer requires the segmentation of the buffer zones into sectors which allows for a spatial arithmetic method to be applied to sum applications by megawatts limited by the boundary condition set out for each satellite and collector's design parameters.

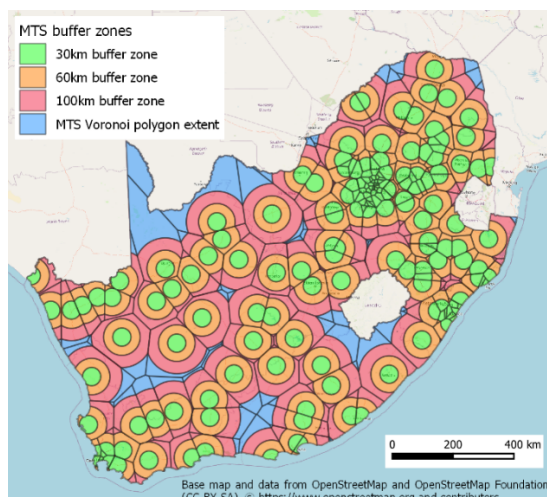


Figure 3: The main transmission stations (MTS) buffer zones with the Voronoi polygon extents

Figure 4 displays the process followed to create the segments in the form of a flowchart. The input datasets for this process were the input stations and the buffer zones, which were created in the last process. The buffer zones were in the correct coordinate system but the input stations needed to be reprojected. Before the processing started, a unique list of station names was extracted from the station's dataset, and was used to iterate through the process to deal with a single station at a time. At the start of the iteration process, the current station and station buffer zone were extracted from the station's dataset. The outer coordinates of the segments were then calculated using the maximum buffer distance from the buffer zones dataset and the number of segments.

$$\theta = \frac{360}{n} \quad (1)$$

$$r = \text{buffer}_{max} \quad (2)$$

where θ = the interior angle of each segment
 n = the number of segments
 $\text{buffer}_{max} = r$ = the maximum buffer distance which is the distance from the station to the outer buffer boundary

Once the base variables were calculated and assigned, the outer coordinates for each segment were calculated using equations 3-6.

$$\Delta x = \sin(\theta \cdot i) \cdot r \quad (3)$$

$$x = \varphi + \Delta x \quad (4)$$

$$\Delta y = \cos(\theta \cdot i) \cdot r \quad (5)$$

$$y = \lambda + \Delta y \quad (6)$$

where Δx = the difference in latitude between the station and segment coordinates
 Δy = the difference in longitude between the station and segment coordinates

i = the segment number (0, 1, 2 etc.)

φ = the latitude of the station

λ = the longitude of the station

x = the latitude of the segment

y = the longitude of the segment

In order to join the coordinates calculated using equations 3 and 6, the current station was buffered by the maximum buffer distance and the outer boundary of this buffer was converted to a line. The coordinates calculated in equations 3 and 6 were then used to create "spoke" lines, which were lines from the station coordinate to the outer boundary coordinates. The spoke lines were merged with the outer boundary line and the resultant lines were converted to polygons to obtain the segments. An intersection was then performed between the new polygon segments layer and the extracted buffer zones for the current station to get the buffer zones and Voronoi polygon shape of the station. The result of the intersection was sanitised by removing duplicates and areas that fell outside of the buffer zone which returned the final buffer zone segments for the current station. This process was repeated for each substation and the segments were exported to a final buffer zone segments dataset. Figure 5 displays a map of the results using the main transmission stations as the input stations and six as the number of segments.

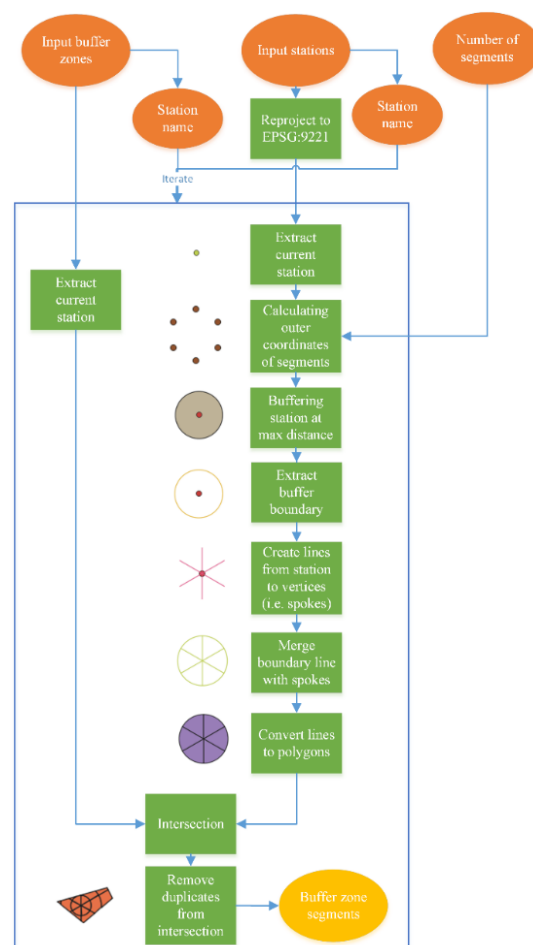


Figure 4: The process flow used to create the buffer zone segments

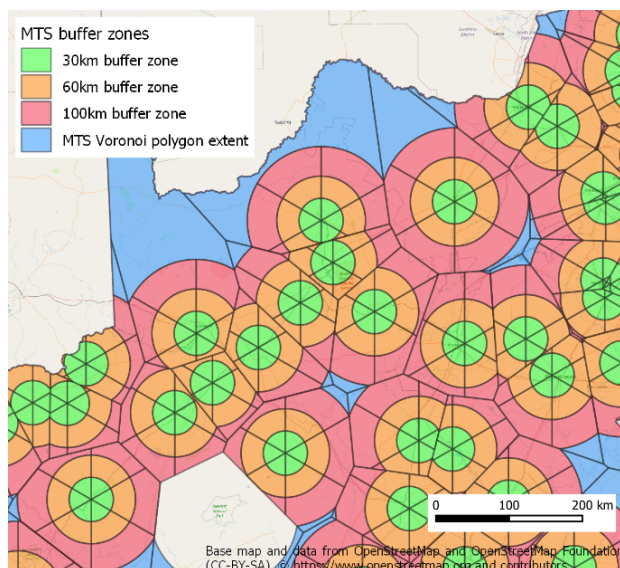


Figure 5: The main transmission stations (MTS) buffer zones segmented into six sectors

3.5 Joining the prospective IPPs to the buffer zone segments

The REEA dataset that was dealt with earlier in this paper was incorporated into the analysis after the creation of the buffer zone segments. The REEA dataset that was processed as described was used to model prospective IPPs. Apart from the REEA dataset, the other input datasets used in this step in the analysis were the input stations, the buffer zones created in 3.3 and the buffer zone segments created in 3.4.

Figure 6 shows the process followed joining the buffer zone segment attributes to the REEA dataset features. Before any processing, all datasets were reprojected to EPSG:9221 so that they are in the same coordinate system. The buffer distances were also extracted from the buffer zones layer and these were used to iterate through the buffer zone segments. This iteration was necessary so that there is no overlap between buffer zones in the analysis. The iteration starts with the lowest buffer zone and moves onto the next lowest distance with each iteration. When the iteration starts, the buffer zone segments were extracted for the current buffer distance and a spatial join performed with the REEA dataset in order to join the station, buffer and segment attributes to the IPP. For the spatial join, the matching features from each iteration were exported while the non-matching features were used as input for the next iteration step. This was to ensure that there were no duplicate IPPs exported. After being exported, the distance between the IPP and the station are calculated as an additional attribute and the features are all saved in a new layer. The IPP features that weren't joined to any buffer zone after the last iteration were then export and the distance to the nearest station calculated. Figure 6 shows the process followed joining the buffer zone segment attributes to the REEA dataset features. The results of this process were modelled using the main transmission stations as the input stations and are shown in Figure 7.

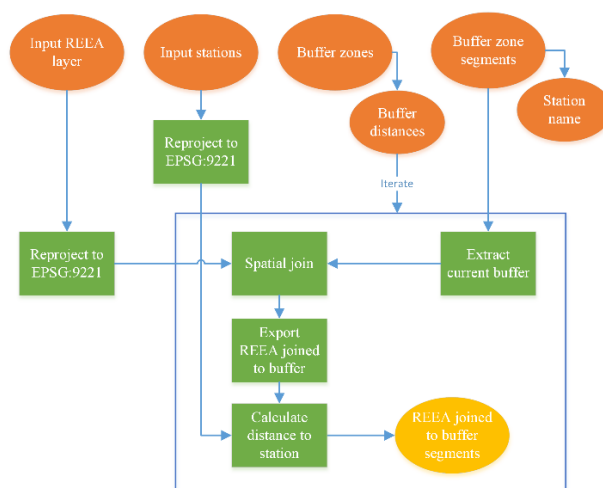


Figure 6: The process flow used to join the REEA dataset to the buffer zone segments

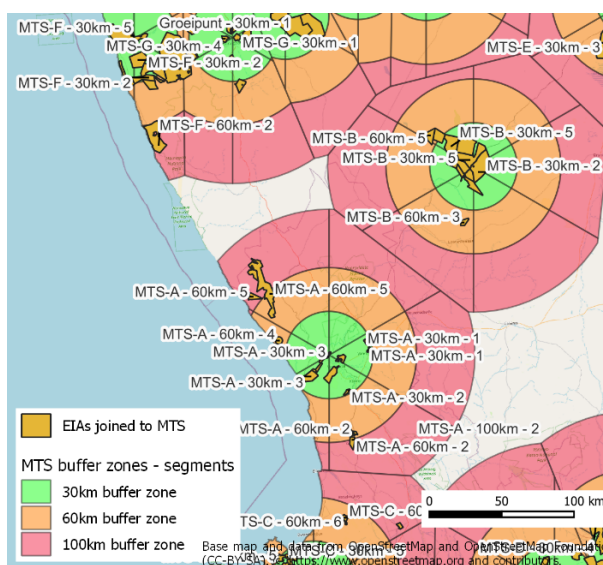


Figure 7: The Renewable Energy EIA Applications (REEA) dataset joined to the buffer zone segments

3.6 Clustering the prospective IPPs by station and capacity

Building on the larger toolset, the final tool addressed in this study was built to cluster the IPPs that were joined to a station in the previous section 3.5. A new clustering was developed as there are no native or plugin tools available in QGIS to cluster based on proximity and a numerical attribute value. This clustering was done using station name, buffer zone and segment ID (the modelling of the proximity) as well as the capacity to be installed at each IPP (the numerical attribute value) using the collector strategy described in section 3.1 of this paper.

The IPP clustering process is shown in Figure 8. The input datasets for this process are the output IPPs dataset from section 3.5, the input stations and the buffer zone segments created in section 3.4. There are two separate iterations that occur at the start of the process. The first iterates on the input station name so that the process deals with a single station at a time. During this iteration, the IPPs from the REEA dataset are extracted for the current station. Within

the first iteration, there is a second that iterates on both the buffer zones and the segment IDs. The purpose of the second iteration is to produce a dictionary within python that summaries the megawatts from IPPs per segment ID and buffer zone as well as just per segment ID. These dictionaries are used when mapping the collector stations – as the segments are grouped into pairs depending on the amount of megawatts per segment. The segment ID with the highest megawatts is selected first, with the next highest adjacent segment paired with it. The segments are then sorted along these lines, pairing segments until each segment is assigned to another as a pair. It was decided to deal with segments as pairs as this decreases the area covered by a collector. Therefore, a collector could only connect to IPPs across two segments within a buffer zone.

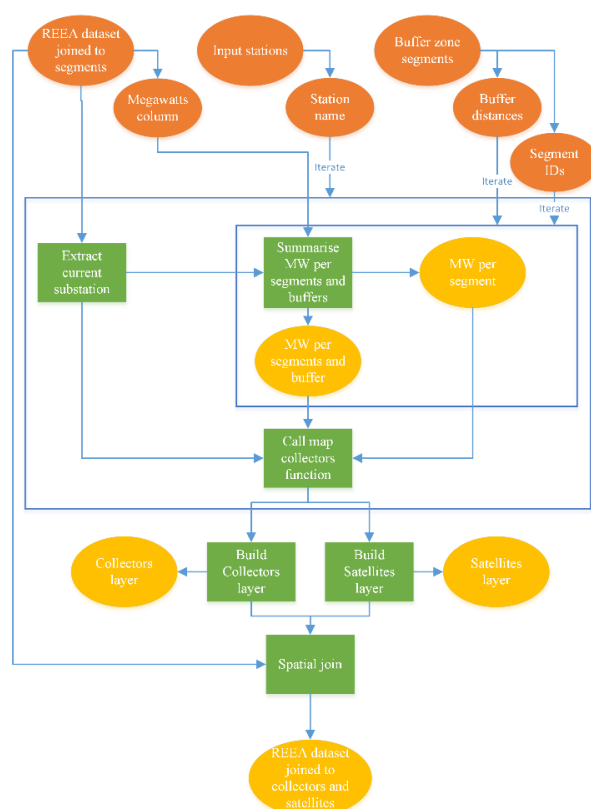


Figure 8: The flow for the master clustering process that clusters IPPs in order to map collector and satellite stations

Once the segments are paired, the “call map collectors” function is invoked. This function is illustrated in Figure 9. The function takes the IPPs extracted for the current station and the megawatt values per segment and buffer as input parameters. It operates by first taking the megawatts value of the smallest buffer zone (e.g. 30km) and the segment with the largest megawatts (e.g. segment ID 1) and testing this to see if the megawatts value of this is larger than 500MW. If it is larger, then the function calls the “map collectors” function. If it is smaller than 500MW, the function checks that there are still segments and buffers remaining with megawatt values and if this is true, it adds the next segment ID for the current buffer zone (e.g. segment ID 2 in 30km buffer zone, then segment ID 1 in

60km buffer zone etc.). If there are no segments and buffer zones with megawatt values left, the function saves the current IPPs as a single collector by calculating the average of the IPP centroid coordinates.

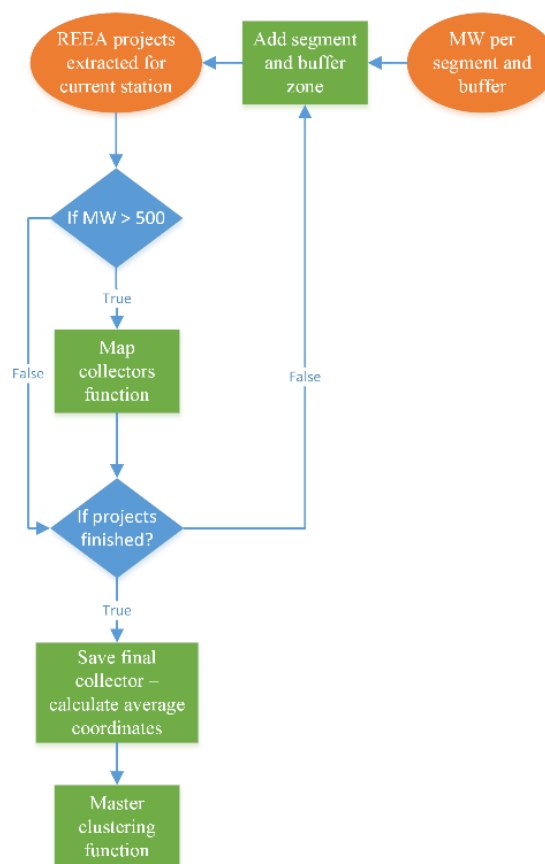


Figure 9: The flow process for the “Call map collectors” function

The “map collectors” function, shown in Figure 10, is called during the “call map collectors” function as described. The “map collectors” function deals with the actual mapping of the collector stations. When called, the function accepts two arguments which are the IPPs extracted for the current segments and buffers. The first step in the process is to create a spatial index using the IPPs which allows for the ability to perform nearest neighbour analysis on the features. The spatial index then selects the first feature in the list of features, and removes it from the spatial index so that it doesn’t find itself during the nearest neighbour analysis, and computes that this feature’s attribute has less than 500 megawatts. If this is the case, a nearest neighbour analysis is performed to find the closest feature – after removing the selected feature from the spatial index – and this process is iterated over until either the list of IPPs is finished or the combined megawatts of the selected IPPs is greater than 500MW. When either condition is true, the collector station is mapped by calculating the average of the centroid coordinates from the list of IPPs selected. After the collector is mapped, there is a check to see if there are any IPPs left and if this is true, the process is started again using the same spatial index to map the next collector. Mapping satellite stations

operate the same way as collectors but only IPPs within or greater than the 60km buffer zone are considered and the maximum megawatts before finalising a satellite station is 250MW. After considering all IPPs, the function returns to the “call map collectors” function. When returned, either the next segment and buffer zone is started or if there are none left, all the collectors and satellites are finalised and numbered and the process returns to the master clustering algorithm shown in Figure 8.

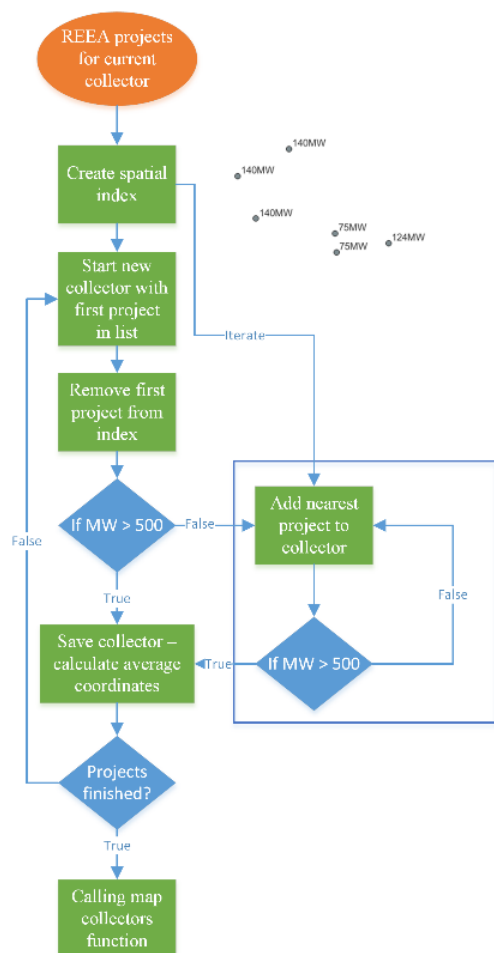


Figure 10: The process flow for the "Map collectors" function

Once all the substations have been iterated over and the collector and satellite stations mapped, the algorithm exits the iteration and starts mapping the collector and satellites stations to new datasets. The new collector and satellite station layers are used to create a layer showing the IPPs joined to the respective collector or satellite station in order for the Network Planner to accurately display these in a map after the analysis. Figure 11 demonstrates the mapped results of the clustering process.

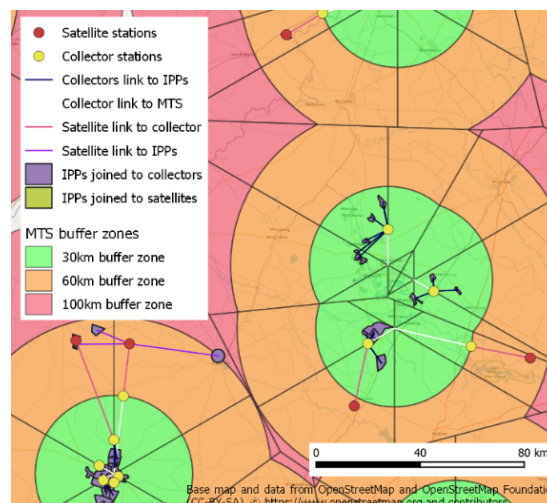


Figure 11: The results of the clustering process modelled on the main transmission stations (MTS) - showing the collector and satellite stations joined to the IPPs and the MTS

4. Discussion

In this paper, a methodology for integrating multiple renewable energy power producers was introduced. The method employs the DFFE’s REEA dataset which is a good indication of possible renewable energy sites. There were limitations with this dataset, as discussed in section 2.1, and these limitations were discussed with the government department to improve the dataset. Of specific concern were duplicates in the dataset and creating a unique identifier for each project area, which will be addressed in future releases.

QGIS was used to create the toolset for this study. In section 3.2, the QGIS Graphical Modeller was initially used to build the functionality but the limitations of iterations forced the use of PyQGIS instead. However, due to the complexity of the tools required – as outlined in section 3.6 – the move to Python was inevitable to leverage on the flexibility in the Python libraries. The option to develop completely outside of QGIS in a pure python environment was considered but the need for Network Planners to use QGIS as a visualisation platform advocated for the continued use of PyQGIS.

The tools created were also built to allow the user flexibility to change parameters that configured the tool’s functionality – something evident in section 3.3 with the buffer distances. This allows the Network Planner to adjust the input parameters to suit their specific area of interest. In section 3.4, creating the boundary vertices for the segments were initially done using the buffer tools and changing the “SEGMENTS” setting. However, this proved inconsistent when changing the “SEGMENTS” setting therefore it was decided to use trigonometric functions to obtain the coordinates of the vertices and join them together. This shift has proved reliable for different segment values.

Performing the spatial join in section 3.5 was the easiest way to join the attribute information from the buffer zone segments to the prospective IPPs. The IPPs were also joined to the buffer zone segment with the largest overlap

however the Network Planner would be free after running this tool to manually change the join for individual IPPs as they see fit. The clustering tool described in section 3.6 took the majority of the time to build. At the moment, the strategy employed in this section is grouping segments together in pairs to ensure that collectors are mapped to IPPs in close proximity. This will be monitored in future along with other restrictions utilised in order to make sure that they are relevant for the collector strategy. This study is a continuously evolving process as more knowledge is gained through connecting renewable energy to the grid.

5. Conclusion

This methodology forms part of a developing technology toolset to assist Network Planning and Designing move away from the classical thinking based on a vertically-integrated passive power model to a deregulated active power flow. The transition from the classical passive model to active integration model is being pushed by the energy transition occurring around the globe. It is an important paradigm shift for transforming a power system from a fossil fuel energy generation to a distributed renewable energy model. This toolset will enable utilities to improve their strategic and long-term plans of connecting a vast number of renewable energy applications as the world decarbonises, digitalises, deregulates and decentralises. This model will assist future Planners to ensure an orderly and organised release of capital expansion projects to ensure grid reliability and resilience of the utility's power system during the transition.

6. Acknowledgments

The authors acknowledge the head of the Planning and GIS departments and the respective management of the Planning and GIS centres of excellence (COE's), for their support during the technology development phases of this project. Their support encourages innovation and value adding to the technology leadership that the COE provides to the wider Distribution business.

7. References

- Asif, M., 2022. The 4Ds of Energy Transition: Decarbonization, Decentralization, Decreasing Use, and Digitalization. John Wiley & Sons.
- Ayamolowo, O.J., Manditereza, P.T., Kusakana, K., 2022. South Africa power reforms: The Path to a dominant renewable energy-sourced grid. *Energy Rep.*, 2021 The 8th International Conference on Power and Energy Systems Engineering 8, 1208–1215. <https://doi.org/10.1016/j.egyr.2021.11.100>
- Bolstad, P., 2008. *GIS Fundamentals: A First Text on Geographic Information Systems*, 3rd ed. College of Food, Agriculture and Natural Resources Sciences, University of Minnesota, St. Paul, MN, USA.
- Chan, H.-Y., Merdekawati, M., Suryadi, B., 2022. Bank climate actions and their implications for the coal power sector. *Energy Strategy Rev.* 39, 100799. <https://doi.org/10.1016/j.esr.2021.100799>
- Covert, T., Greenstone, M., Knittel, C.R., 2016. Will We Ever Stop Using Fossil Fuels? *J. Econ. Perspect.* 30, 117–138. <https://doi.org/10.1257/jep.30.1.117>
- Department of Environmental Affairs, 2013. Draft National Renewable Energy Guideline. Department of Environmental Affairs, Pretoria, South Africa.
- Department of Mineral Resources and Energy, 2019. Integrated Resource Plan. Department of Mineral Resources and Energy, Pretoria.
- DFFE, 2022. Renewable Energy [WWW Document]. URL https://egis.environment.gov.za/renewable_energy (accessed 12.5.22).
- Eskom, 2021. Integrated Report. Eskom Holdings SOC Ltd, Johannesburg.
- Floors, R., von Saint Ange, U., 2021. High-Resolution Wind Resource Map for South Africa 2020.
- IPCC, 2022. Climate Change 2022: Impacts, Adaptation, and Vulnerability. Contribution of Working Group II to the Sixth Assessment Report of the Intergovernmental Panel on Climate Change [H.-O. Pörtner, D.C. Roberts, M. Tignor, E.S. Poloczanska, K. Mintenbeck, A. Alegria, M. Craig, S. Langsdorf, S. Löschke, V. Möller, A. Okem, B. Rama (eds.)]. Cambridge University Press, Cambridge University Press, Cambridge, UK and New York, NY, USA.
- Jaglal, P., 2016. Sub-Transmission Building Blocks for IPP Integration. Eskom Holdings SOC Ltd, Johannesburg.
- Mashishi, N., 2021. South Africa the 12th biggest source of greenhouse gases? Yes, but that's not the only measure that matters [WWW Document]. URL <https://www.polity.org.za/article/south-africa-the-12th-biggest-source-of-greenhouse-gases-yes-but-thats-not-the-only-measure-that-matters-2021-04-19> (accessed 5.4.23).
- Matshidza, D., Satimburwa, S., Dlamini, B., 2022. Transmission Generation Connection Capacity Assessment of the 2024 Transmission Network (GCCA - 2024). Eskom Holdings SOC Ltd, Johannesburg.
- Naicker, P., Thopil, G.A., 2019. A framework for sustainable utility scale renewable energy selection in South Africa. *J. Clean. Prod.* 224, 637–650. <https://doi.org/10.1016/j.jclepro.2019.03.257>
- Suri, M., Betak, J., Rosina, K., Chrkavy, D., Suriova, N., Cebecauer, T., Caltik, M., Erdelyi, B., 2020. Global-Photovoltaic-Power-Potential-by-Country.pdf [WWW Document]. *Glob. Photovolt. Power Potential Ctry.* URL <https://documents1.worldbank.org/curated/en/466331592817725242/pdf/Global-Photovoltaic-Power-Potential-by-Country.pdf> (accessed 11.25.22).
- World Bank, 2022. World Bank Approves \$497 Million in Financing to Lower South Africa's Greenhouse Gas Emissions and Support a Just Transition [WWW Document]. World Bank. URL <https://www.worldbank.org/en/news/press-release/2022/11/04/world-bank-approves-497-million-in-financing-to-lower-south-africa-s-greenhouse-gas-emissions-and-support-a-just-transit> (accessed 11.24.22).